European Journal of Immunology

HIGHLIGHTS

Basic

FRONTLINE | Research Article

Musculin inhibits human T-helper 17 cell response to interleukin 2 by controlling STAT5B activity

Veronica Santarlasci[1], Alessio Mazzoni[1], Manuela Capone[1], Maria Caterina Rossi[1], Laura Maggi[1], Gianni Montaini[1], Beatrice Rossettini[1], Rolando Cimaz[2], Matteo Ramazzotti[3], Giusi Barra[4], Raffaele De Palma[4,5], Enrico Maggi[1], Francesco Liotta[1], Lorenzo Cosmi[1], Sergio Romagnani[1] and Francesco Annunziato[1,6]

[1] Department of Experimental and Clinical Medicine and DENOTHE Center, University of Florence, Firenze, Italy
[2] Anna Meyer Children's Hospital and University of Florence, Italy
[3] Department of Biomedical Experimental and Clinical Sciences "Mario Serio" University of Florence, Firenze, Italy
[4] Department of Clinical and Experimental Medicine, Università della Campania "L. Vanvitelli," Napoli, Italy
[5] Institute of Protein Biochemistry, CNR, Napoli
[6] Regenerative Medicine Unit and Immunology and Cellular Therapy Unit of Azienda Ospedaliera Careggi, Florence, Italy

We recently demonstrated that human T-helper (Th) 17 cells, unlike Th1 cells, do not proliferate in response to T-cell receptor stimulation, mainly because of their reduced capacity to produce and respond to IL-2. In this study, we show that their lower responsiveness to IL-2 is due to the selective expression of Musculin (MSC), a member of the basic helix-loop-helix transcription factors. We show that MSC expression in human Th17 cells is retinoic acid orphan receptor (ROR)γt-dependent, and allows the upregulation of PPP2R2B, a regulatory member of the protein phosphatase 2A (PP2A) enzyme. High PPP2R2B levels in human Th17 cells were responsible for the reduced STAT5B Ser-193 phosphorylation upon IL-2 signalling and, therefore, impaired STAT5B DNA binding and transcriptional activity on IL-2 target genes. PP2A, observed in Th17 cells, controls also STAT3, dephosphorylating Ser727, thus increasing its activity that plays a crucial role in Th17 development and/or maintenance. Thus, our findings identify an additional mechanism responsible for the limited expansion of human Th17 cells, and could provide a further explanation for the rarity of these cells in inflamed tissues.

Keywords: IL-2 · Musculin · Proliferation · RORC · STAT5 · Th17

Additional supporting information may be found in the online version of this article at the publisher's web-site

Introduction

The decision of a naïve $CD4^+$ T-helper (Th) cell to acquire a particular effector phenotype is dictated by the cytokines produced by cells of the innate immunity in response to microbes and the consequent activation of transcription factors. In the presence of

Correspondence: Prof. Francesco Annunziato
e-mail: francesco.annunziato@unifi.it

IL-12, naïve T cells activate signal transducer and activator of transcription 4 (STAT4) and T-bet, which induce the production of IFN-γ (Th1 cells); in the presence of IL-4, naïve T cells activate STAT6 and GATA-3, which stimulate the production of IL-4, IL-5, and IL-13 (Th2 cells); finally, in the presence of IL-1β and IL-23, naïve T cells activate STAT3 and retinoic acid orphan receptor (ROR)γt that allow them to produce IL-17 (Th17 cells). Th1 cells activate in turn macrophages, NK cells and B cells and play an important role in the protection against intracellular microbes, but they have also been thought to play a pathogenic role in autoimmune disorders. Th2 cells activate eosinophil granulocytes, mast cells, basophils, as well as the production of IgE by B cells, thus contributing to the protection against extracellular parasites, venoms and irritants, but they can also be responsible for atopic disorders. Th17 cells activate macrophages, B cells and also neutrophil granulocytes, thus favoring the protection against extracellular microbes. These cells seem to play an even more important pathogenic role than Th1 cells in autoimmune diseases [1]. However, despite their probably powerful pathogenicity, human Th17 cells have been found to be very rare in the inflammatory tissues of different chronic inflammatory disorders, such as the skin of patients with psoriasis, the synovial fluid (SF) of joints from patients with juvenile idiopathic arthritis (JIA), the gut of patients with Crohn's disease (CD) [2]. In the last years, we have extensively investigated the reasons for the rarity of Th17 cells in inflammatory sites and have identified some of them. One of these is surely their rapid ability to shift into Th1 cells in the presence of inflammatory cytokines, such as IL-12 [3] and TNF-α [4]. These Th17-derived Th1 cells have been named as nonclassic Th1 cells to distinguish them from the classic Th1 cells that instead originate directly from CD4+ naïve T cells in response to IL-12 produced by dendritic cells, and the distinctive phenotypic and epigenetic features of the two types of Th1 cells have been described [5–7]. Another important reason is their limited expansion in response to either T-cell receptor (TCR) triggering by antigen-stimulation and/or to the most important T-cell growth factor, IL-2. In a previous study, we have demonstrated that human Th17 cells express high levels of IL-4-induced gene I (IL4I1), which inhibits the CD3-dependent pathway of IL-2 production [8]. In the same study, the reduced IL-2 responsiveness was explained by the lack of PI3K-AKT-mTORC1 axis activation, with a reduced S6ribo phosphorylation, but the mechanisms involved in this defect were not fully investigated [8].

In the present study, we tried to better clarify the mechanisms responsible for the poor responsiveness of human Th17 cells to IL-2. To do this, we utilized a microarray analysis performed on a set of human Th17 and Th1 clones, which has already been reported [8]. Among the genes that fulfilled the criteria as upregulated in Th17 versus Th1 cells, there was musculin (MSC), a member of the basic helix-loop-helix transcription factor family. MSC, also named as Myogenic repressor (MyoR) or Activated B cell factor-1 (ABF-1) was first identified in mouse skeletal muscle precursors, but also in Hodgkin lymphomas, in Epstein-Barr virus-transformed B-cell lines and more recently in murine follicular T-helper (Tfh) cells. MSC has been shown to form heterodimers with E proteins and acts as a potent transcriptional repressor that blocks activation of E-box-dependent genes. However, the functional role of MSC in T lymphocytes had not yet been clarified. We first found that MSC expression in human Th17 cells was RORγt-dependent and, more importantly, that the forced MSC expression in either Th1 clones or ex vivo isolated Th1 cells inhibited their responsiveness to IL-2. Moreover, the results of our study also showed that MSC acts on STAT5B ser193 phosphorylation. This phenomenon was obtained by directing the activity of the protein phosphatase 2A (PP2A) on STAT5B ser193 through the expression of the PP2A regulatory subunit PPP2R2B.

Results

MSC is expressed by both human Th17 clones and ex vivo isolated IL-17-producing cells

In this study, we further assessed differences between human Th17, Th17/Th1, classic, and nonclassic Th1 cells with regard to the expression of genes potentially involved in cell activation in response to six hours of anti-CD3 mAb plus anti-CD28 mAb stimulation. To do this, we took advantage of a transcriptome analysis already reported and performed on a panel of human Th17 and Th1 clones stimulated with anti-CD3 and anti-CD28 mAb [8]; among the genes upregulated in Th17 versus Th1 clones there was *MSC*, a member of the basic helix-loop-helix transcription factors [9–12]. In order to confirm transcriptome data, Th17, Th17/Th1, classic, and nonclassic Th1 clones derived from peripheral blood (PB) of healthy subjects were subjected to stimulation with anti-CD3 plus anti-CD28 mAb and MSC mRNA expression was analyzed by quantitative RT-PCR. As shown in Fig. 1A, MSC mRNA levels were higher in Th17 than in classic Th1 clones, while Th17/Th1 and nonclassic Th1 clones showed intermediate expression levels. Anti-CD3 plus anti-CD28 mAb stimulation did not significantly affect MSC mRNA expression in any of Th clones analyzed (Fig. 1A). Accordingly, Western blot and confocal microscopy analysis confirmed the selective expression of MSC in Th17 as compared with that in classic Th1 clones in resting conditions (Fig. 1B and C). Stable gene expression or inhibition is often accompanied by epigenetic remodeling of the gene locus through DNA methylation and/or histone modifications. Thus, in order to evaluate the stability of *MSC* mRNA expression or inhibition in Th17 and classic Th1 cells, respectively, we decided to investigate the DNA methylation pattern of this locus. *MSC* gene has a CpG island spanning the first exon, thus we analyzed by bisulfite cloning and sequencing several portions of this region, but we always observed a complete demethylation in both cell subsets (data not shown). By contrast, when we moved our attention to a region located 500 bp upstream of the transcriptional start site, we observed a different methylation pattern, with Th17 cells being demethylated, and classic Th1 cells, on the opposite, highly methylated (Fig. 1D).

In order to exclude the possibility that MSC selective expression by Th17 cells was due to an artefact resulting from

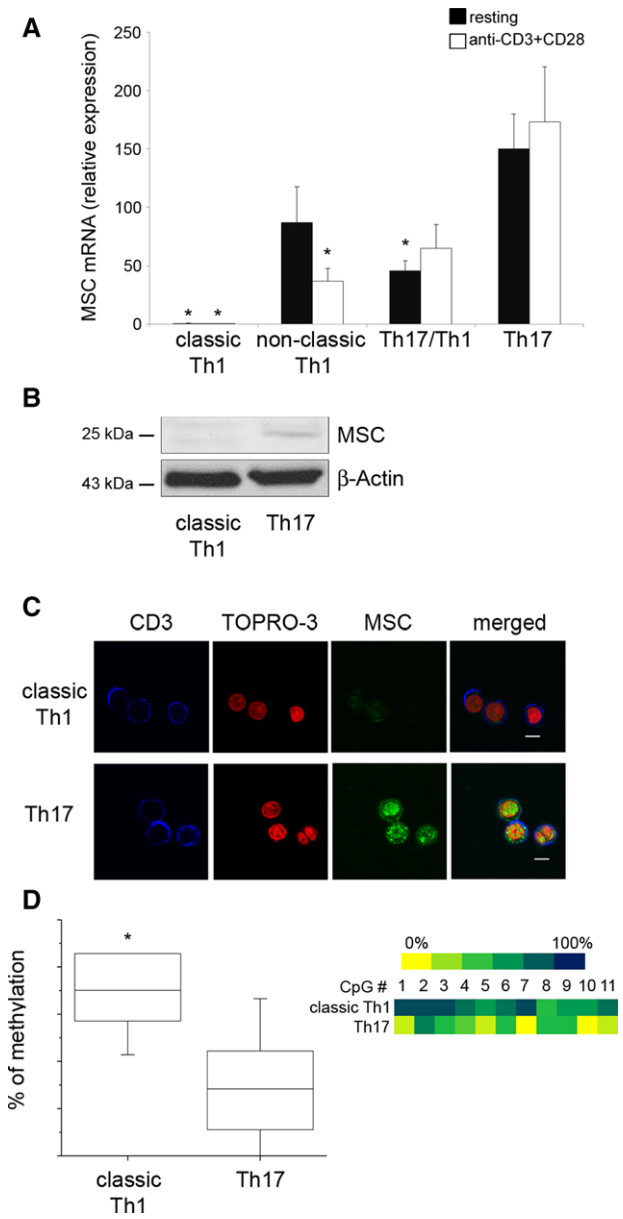

Figure 1. Musculin is selectively expressed by human Th17 cells (A) real-time quantitative PCR evaluation of Musculin gene expression in resting and stimulated for 6 h with anti-CD3-CD28 mAbs classic Th1, nonclassic Th1, Th17/Th1, and Th17 cell clones ($n = 21$ clones for each phenotype). Data are presented as mean of mRNA expression (normalized on GAPDH) + SE. Statistical analysis was performed for all phenotypes versus Th17 using Student's unpaired *t*-test: $^{*}p \leq 0.01$. (B, C) Musculin expression was evaluated at protein level on three different classic Th1 and three different Th17 clones by both (B) Western blot (a representative blot of one of the clones analyzed is shown) and (C) confocal microscopy analysis (one representative experiment, out of three, is shown, scale bars 5 μm). (D) DNA methylation status of Musculin gene in classic Th1 and Th17 cell clones is represented with a colorimetric-code (yellow-blue scale). Methylation levels at each CpG site is the average of three cell clones (right). The distribution of the average methylation levels at each CpG site of the whole region is depicted also as box plot for each population. Means and 25th and 75th percentiles are shown in boxes, and minimum and maximum values are shown as whiskers (left of the panel). Statistical significance was determined using Mann–Whitney *t*-test: $^{*}p \leq 0.05$.

the use of long-term in vitro cultured T cells (T-cell clones), *MSC* mRNA levels were also measured in ex vivo-derived CD161+CCR6+IL^{-}17+IFN-γ^{-} (Th17), CD161+CCR6+IL-17-IFN-γ+ (nonclassic Th1), and CD161^{-}CCR6^{-}IL-17-IFN-γ+ (classic Th1) cell subsets, which had been purified from circulating CD4^{+} T cells by FACS following the cytokine secretion assay, as already reported [7]. In agreement with data obtained using T-cell clones, ex vivo-derived Th17 cells expressed higher levels of MSC mRNA than classic cells (Supporting Information Fig. 1). Similar data were obtained isolating the above indicated cell subsets from the PB and SF of two JIA affected patients, indicating that also under inflammatory conditions MSC associates with Th17 cells (data not shown).

RORγt directly regulates MSC expression in CD4^{+} T cells

To establish whether the high MSC expression in Th17 cells was RORγt-dependent, the existence of a possible correlation in the expression of the two molecules was evaluated. As shown in Fig. 2A, there was a strict positive correlation between mRNA expression of *RORC2* (which encodes RORγt) and *MSC*. This observation prompted us to investigate whether RORγt was directly involved in *MSC* expression. PCR analysis performed on DNA from Th17 cell clones precipitated with an anti-RORγt Ab, clearly demonstrated the existence of a direct interaction between RORγt and the *MSC* gene (Fig. 2B). Moreover, in order to directly demonstrate that the increased *MSC* expression in Th17 cells was RORγt dependent, classic Th1 clones, and naïve umbilical cord blood (UCB) CD4^{+}CD161^{-} cells were transduced with *RORC2*- or control-lentivirus and then assessed for *MSC* mRNA expression. As expected, all Th1 clones and naïve UCB CD4^{+}CD161^{-} cells transduced with *RORC2* showed higher expression of *RORC2* mRNA compared to cells transduced with empty vector (data not shown). Moreover, *RORC2*-transduced cells, both Th1 clones (Fig. 2C) and UCB CD4^{+}CD161^{-} cells (Fig. 2D), had higher *MSC* mRNA expression in comparison with their empty vector-transduced counterparts. On the other hand, gene-targeting of *RORC2* expression in Th17 clones, by using *RORC2*-specific small interfering (si)RNA, resulted in a marked decrease of both *RORC2* and *MSC* mRNA expression (Fig. 2E).

Transduction of MSC in CD4^{+} T cells reduces their ability to proliferate in response to IL-2

Once we established that MSC was selectively expressed by Th17 cells and that its expression was directly regulated by RORγt, we started to evaluate its possible functions in CD4^{+} T cells. To this aim, PB-derived CD4^{+}CD161^{-}CCR6^{-}CXCR3^{+} (classic Th1) cells, which express neither *MSC* mRNA nor its protein, were transduced with *MSC*- or control-lentivirus vector and then assessed for *MSC* mRNA and protein expression by quantitative PCR, Western blot, and confocal microscopy, respectively. As shown in Fig. 3A, B, and

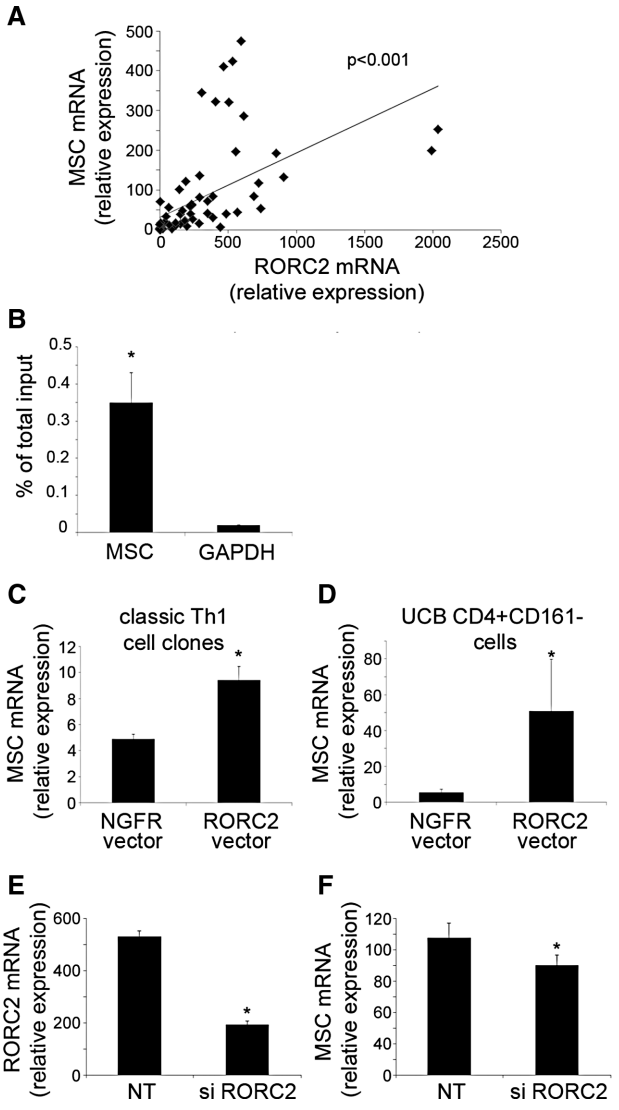

Figure 2. Musculin expression is RORγt dependent (A) correlation between Musculin and RORC2 mRNA levels normalized on GAPDH was performed in Th17, Th17/Th1, classic, and nonclassic Th1 clones ($n = 70$ clones). Statistical significance was determined using Pearson's correlation: $p \leq 0.001$ (B) ChiP was performed with anti-human RORγt on three pools, each comprised of two Th17 cell clones upon 6 h activation with anti-CD3-CD28 mAbs. The immunoprecipitated DNA was amplified by RT-PCR with primers specific for Musculin and GAPDH promoters, and the results are expressed as ΔΔCt compared with no-Ab input material used as control, and then plotted as percentage of total input. Statistical significance was determined using Mann–Whitney *t*-test: $^{*}p \leq 0.05$. (C) Real-time PCR evaluation of Musculin mRNA expression in three RORC2 and NGFR-control transduced classic Th1 cell clones. (D) Real-time PCR evaluation of Musculin mRNA expression in three RORC2 and NGFR-control transduced umbilical cord blood CD4+CD161- cell lines. (C, D) Data are presented as mean of mRNA expression (normalized on GAPDH) + SE. Statistical significance was determined using Student's paired *t*-test: $^{*}p \leq 0.05$. (E, F) Evaluation of mRNA expression of (E) RORC2 and (F) MSC in three different Th17 cell clones after 72 h transfection with RORC2-specific siRNA and control (NT)-siRNA. $^{*}p \leq 0.05$. Data are presented as mean of mRNA expression (normalized on GAPDH) + SE. Statistical significance was determined using Student's paired *t*-test: $^{*}p \leq 0.05$.

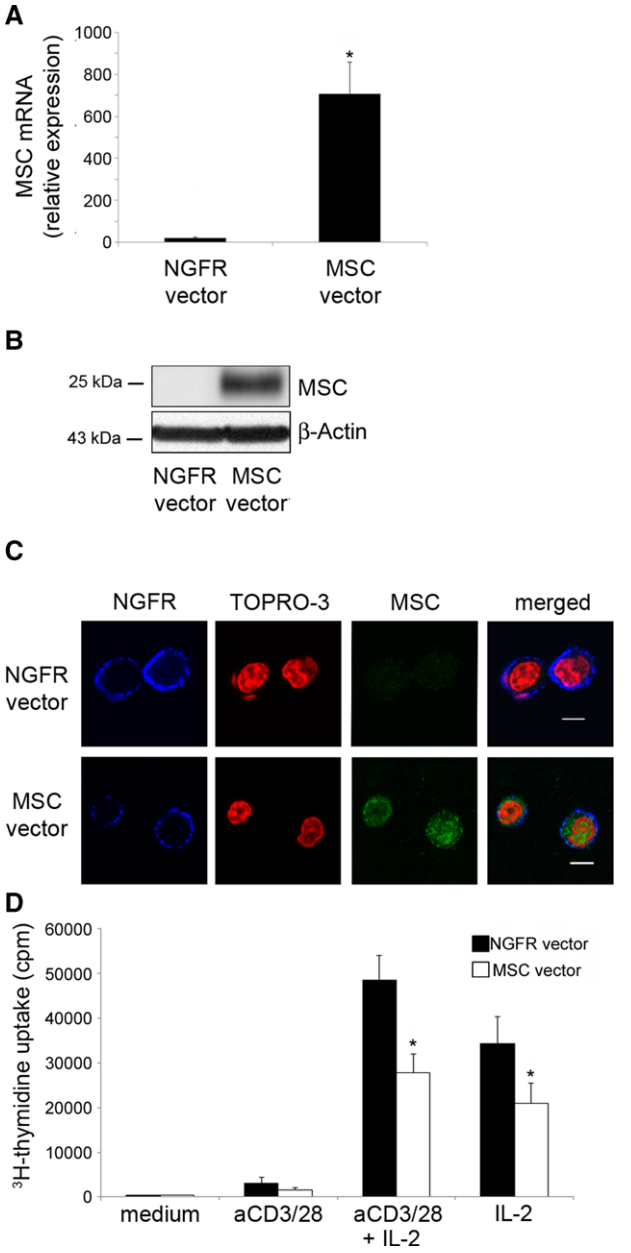

Figure 3. Musculin overexpression in classic-Th1 cells dampens their IL-2 induced proliferation (A) real-time PCR evaluation of Musculin mRNA expression in 10 Musculin and NGFR-control transduced classic Th1 cell lines. Data are presented as mean of mRNA expression (normalized on GAPDH) + SE. Statistical significance was determined using Student's paired *t*-test: $^{*}p \leq 0.01$. (B, C) Upregulation of Musculin expression was evaluated also at protein level by (B) Western blot and (C) confocal microscopy analysis (scale bars 5 μm). Single representative experiments are shown. (D) 10 NGFR-control (black columns) and Musculin- (white columns) transduced classic Th1 cell lines were cultured with anti-CD3-CD28 mAbs for 3 days, in the absence or presence of IL-2, or with IL-2 alone. Proliferative response was assessed at day 3 by ^{3}H-TdR uptake. The mean values of cpm+SE are reported. Statistical significance was determined using Student's paired *t*-test, Musculin versus NGFR-control: $^{*}p \leq 0.001$.

C, *MSC*-, but not control-lentivirus transduction, induced high *MSC* mRNA and protein expression by PB-derived classic Th1 cells.

In a previous study, we showed that Th17 cells, unlike Th1 cells, exhibit poor or no proliferation because of at least two reasons: (i) an impairment to produce IL-2 in response to anti-CD3 plus anti-CD28 stimulation and (ii) a reduced ability to respond to IL-2 [8]. The reduced IL-2 responsiveness was explained by the lack of PI3K-AKT-mTORC1 axis activation, whereas the defective IL-2 production by Th17 cells appeared to be related to their reduced c-Fos, c-Jun, and nuclear factor of activated T cells activity. The reduced activity of these transcription factors associated with high expression of the IL-4-induced gene 1 (*IL4I1*) mRNA, which encodes for a L-phenylalanine oxidase that has been shown to downregulate CD3ζ expression in T cells [8]. For this reason, we decided to investigate whether MSC could also be involved in one or both these pathways. Thus, MSC- and control-lentivirus transduced cells were tested for their ability to proliferate in response to anti-CD3 plus anti-CD28 mAb stimulation, in the presence or in the absence of exogenous recombinant IL-2. As shown in Fig. 3D, MSC-lentivirus transduced cells showed a nonsignificant reduction of the proliferation induced by anti-CD3 plus anti CD28 mAb as compared to control-lentivirus transduced ones. In agreement with these data suggesting that MSC might not be involved in affecting TCR signaling, no significant differences of *IL4I1* mRNA and CD3ζ and CD3ε protein expression were detected between MSC- and control-lentivirus transduced cells (Supporting Information Fig. 2A, B, and C). Moreover, comparable CD3ζ pTyr142 phosphorylation levels were achieved in *MSC*- and control-lentivirus transduced cells upon anti-CD3 plus anti-CD28 stimulation (Supporting Information Fig. 2D). By contrast, the cell response to IL-2, both in absence or presence of contemporary TCR and CD28 triggering, was significantly affected by the forced expression of MSC (Fig. 3D). Therefore, we came to the conclusion that high MSC expression in human Th17 cells may associate with their reduced IL-2 response, and we decided to investigate better their IL-2 signaling pathway. IL-2 transduces its signal through the IL-2 receptor (IL-2R) complex, which is made of two essential signaling subunits, IL-2Rβ and IL-2Rγ, and one affinity modulating subunit, IL-2Rα. IL-2-induced heterodimerization of IL-2Rβ and IL-2Rγ results in activation of receptor-associated JAK1 and JAK3 through trans- or auto-phosphorylation [13]. Subsequent tyrosine phosphorylation of the IL-2Rβ chain provides docking sites for effector molecules including STAT5A and STAT5B. Human STAT5A and STAT5B are phosphorylated on the conserved tyrosine (Tyr) residues Tyr694 and Tyr699, respectively, which allows their dissociation from the receptor complex, formation of hetero- or homodimers, and nuclear translocation to bind specific promoter elements that stimulate transcription of target genes that control cell growth and differentiation. In addition to tyrosine phosphorylation, IL-2 induces serine (Ser) phosphorylation of STAT5 and recent data indicate that STAT5B undergoes cytokine-induced phosphorylation at Ser193 through a rapamycin-sensitive mechanism [14, 15].

We started our IL-2 signaling investigation by evaluating the expression of the IL-2 receptor chains but, as shown in Fig. 4A, no significant differences of *ILRA*, *IL2RB*, and *IL2RG* mRNA levels were detectable between MSC- and control-lentivirus transduced classic Th1 cell lines ($n = 10$) . Then, total STAT5A and B, as well as their phosphorylation status at both tyrosine and serine residues, were evaluated in steady state and upon IL-2 stimulation in *MSC*- or control-lentivirus transduced classic Th1 cells. As shown in Fig. 4B, STAT5A/B phosphorylation at Tyr 694/699 in response to IL-2 stimulation was not affected by the forced expression of MSC, as demonstrated by flow cytometric analysis. Instead, both Western blot and confocal microscopy analysis evidenced a significant reduction of STAT5B Ser193 phosphorylation in *MSC*-transduced cells, when compared to the control (Fig. 4C and D). Of note, both Western blot and confocal microscopy analysis showed no differences of total STAT5B protein levels between *MSC*- and control-lentivirus transduced cells (Fig. 4E and F). These data clearly suggest that the reduced STAT5B Ser193 phosphorylation, which characterizes *MSC*-transduced classic Th1 cells, is not due to a reduction of total STAT5B protein expression.

In order to conclude that the effects on IL-2 signaling observed in classic Th1 cells after MSC overexpression reflect the physiological inhibition of this pathway that is present in human Th17 cells, we repeated the previous experiments on both human Th17 and classic Th1 cells. As shown in Supporting Information Fig. 3, in agreement with our previous findings [8] we found no differences in the mRNA expression of the different IL-2 receptor chains (panel A), as well as no differences in STAT5A/B Tyr694/699 phosphorylation upon IL-2 stimulation in both Th17 and classic Th1 cells (panel B). However, in agreement with the data obtained on *MSC*-transduced classic Th1 cells, Th17 cell lines displayed impaired STAT5B Ser193 phosphorylation when compared to classic Th1 cells upon IL-2 signaling (Fig. 5A). Even in this case, the reduced Ser193 phosphorylation could not be ascribed to a lower expression of total STAT5B protein in Th17 cells compared to Th1 cells (Fig. 5B).

Human Th17 cells are characterized by a high level of PPP2R2B expression

Recent data indicate that STAT5B undergoes IL-2-induced phosphorylation at Ser193 through a rapamycin-sensitive mechanism [15]. In addition, the serine/threonine protein phosphatase 2A (PP2A) has been shown to dephosphorylate STAT5B at Ser193 residue reducing its DNA binding and transcriptional activity [15]. We have previously shown that human Th17 cells have reduced activation of the mTOR pathway in response to IL-2 [8], and this may partially account for the reduced phosphorylation of STAT5B Ser193 in response to IL-2. In order to understand how the activity of a transcription factor like MSC could be related to the reduced STAT5B Ser193 phosphorylation, we took advantage again of the gene expression profile obtained by microarray analysis performed on a panel of human Th17 and Th1 clones, looking for differentially expressed protein phosphatases. Among the genes upregulated in Th17 versus Th1 clones we found protein phosphatase 2, regulatory subunit B, beta (*PPP2R2B*). *PPP2R2B* belongs to the

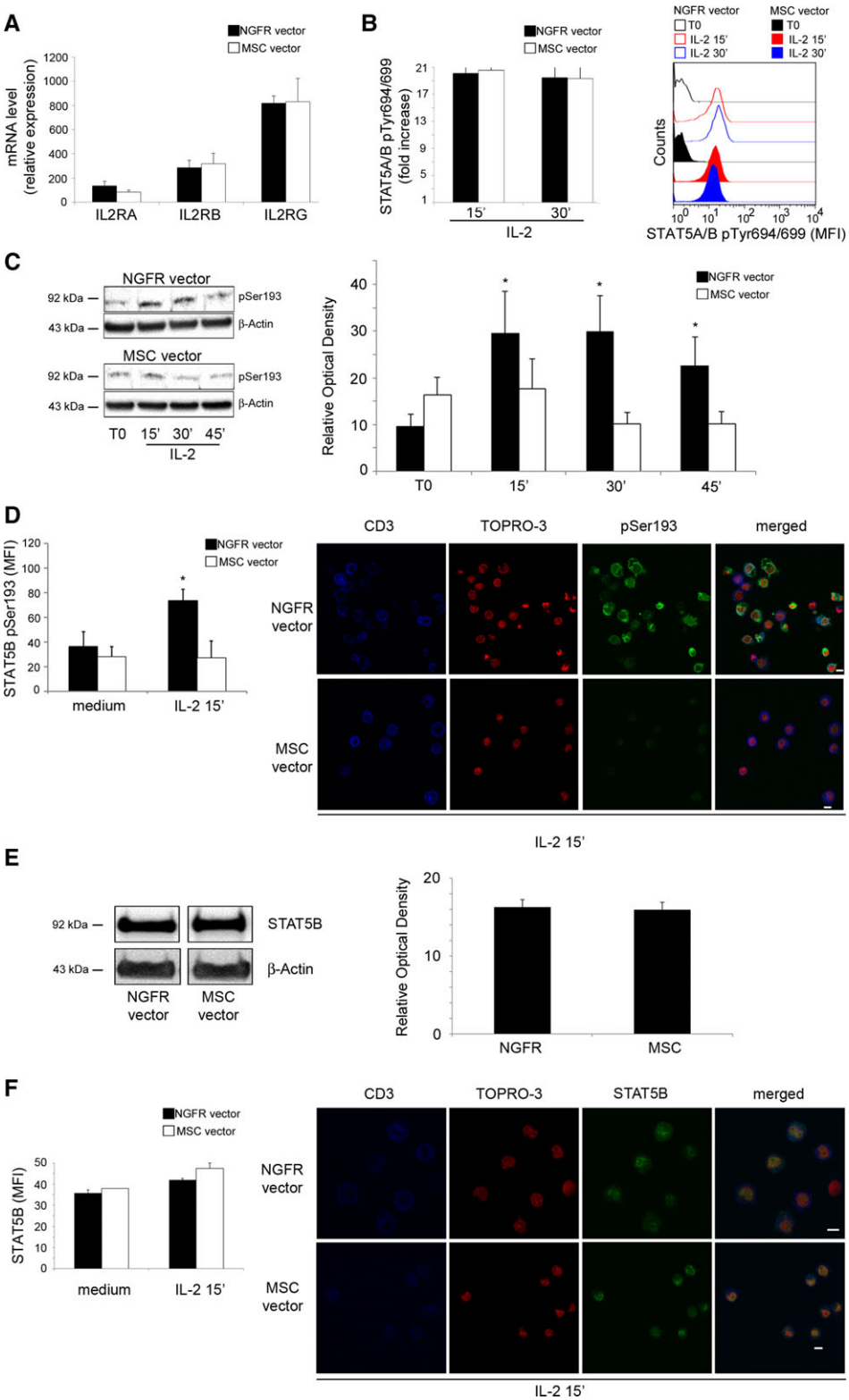

Figure 4. Musculin affects IL-2 signaling by reducing STAT5B Ser193 phosphorylation in MSC-transduced classic Th1 cells 10 classic Th1 cells lines were transduced with either control NGFR vector or MSC-vector and subjected to IL-2 stimulation. (A) Real-time quantitative PCR evaluation of IL-2R chains expression by NGFR control- (black columns) or MSC- (white columns) transduced classic Th1 cells. Data are presented as mean of mRNA expression (normalized on GAPDH) + SE. (B) Phosphorylation of STAT5A/B (Tyr694/699) in NGFR control- (black columns) or MSC- (white columns) transduced classic Th1 cells (n = 10 cell lines) induced by IL-2 stimulation (15′ and 30′), was evaluated by flow cytometry. Results are expressed as fold change of MFI on stimulated versus unstimulated, left panel; a representative histogram analysis is shown on the right panel. (C, D) Phosphorylation of STAT5B (Ser193) in NGFR control- (black columns) or MSC- (white columns) transduced classic Th1 cells (n = 3 cell lines) induced by IL-2 stimulation at the indicated time points, was evaluated by Western blot and confocal microscopy. (C) One representative immunoblot is shown (left); the mean + SE of relative optical density of three independent experiments are depicted (right). Statistical significance, between time points versus time 0, was determined using Student's paired t-test: $^{*}p \leq 0.05$. (D) MFI of confocal microscopy analysis is depicted (left). Statistical significance, stimulated versus unstimulated, was determined using Student's paired t-test: $^{*}p \leq 0.05$. One representative picture is depicted (right, scale bars 5 μm). (E, F) Total STAT5B protein was evaluated by (E) Western blot and (F) confocal microscopy in NGFR control- (black columns) or MSC- (white columns) transduced classic Th1 cells (n = 3 cell lines). (F) Results are expressed as MFI mean + SE.

large family of genes that encode for regulatory subunits of the PP2A phosphatase. PP2A is composed of a scaffold subunit (A), a catalytic subunit (C), and a regulatory (B) subunit. The catalytic and scaffold subunits are each coded by two closely homologous genes (PP2A C α, PPP2CA, and β, PPP2CB; PP2A A α, PPP2R1A, and β, PPP2R1B). In contrast, the regulatory subunits are coded by a large variety of genes that have been grouped in three families (B, B′, and B″). A functional PP2A holoenzyme is formed when the relatively invariant catalytic/scaffold core heterodimer couples with one of the B subunits. The choice of the regulatory B

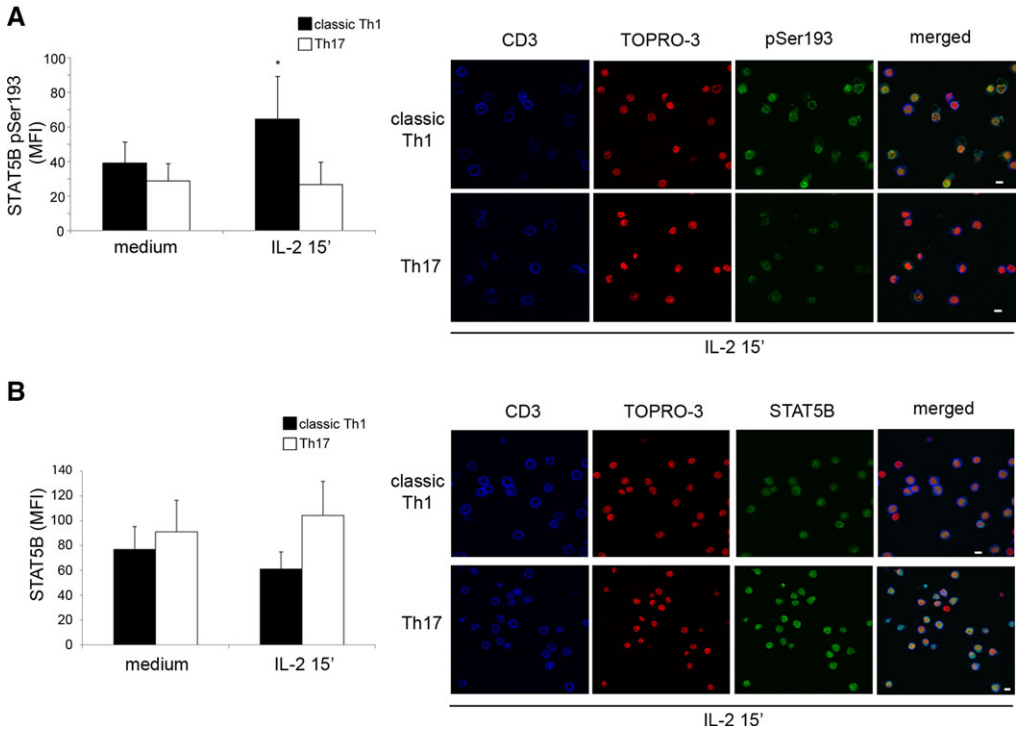

Figure 5. Musculin affects IL-2 signaling by reducing STAT5B Ser193 phosphorylation in Th17 cells STAT5B Ser193 phosphorylation upon IL-2 signaling was evaluated in classic Th1 and Th17 cell lines. (A) Phosphorylation of STAT5B Ser193 in three classic Th1 (black columns) and 3 Th17 (white columns) cell lines induced by 15' IL-2 stimulation, was evaluated by confocal microscopy. Results are expressed as MFI of + SE (left). One representative picture is depicted (right, scale bars 5 μm). Statistical significance was determined using Student's unpaired *t*-test: $^{*}p \leq 0.05$ versus unstimulated cells. (B) Total STAT5B protein was evaluated by confocal microscopy in three classic Th1 (black columns) and 3 Th17 (white columns) cell lines (scale bars 5 μm). Results are expressed as MFI mean +SE (left). One representative picture is depicted (right, scale bars 5 μm).

subunit determines the substrate specificity of the enzyme. By this way, the same enzyme has distinct targets in different cells [16]. Therefore, *PPP2R2B* mRNA expression was analyzed by quantitative RT-PCR on a series of human Th17 and classic Th1 clones derived from PB of healthy subjects. As shown in Fig. 6A, *PPP2R2B* mRNA levels were significantly higher in Th17 than in classic Th1 clones. In order to establish whether the high *PPP2R2B* expression in Th17 cells was RORγt- and MSC-dependent, the existence of a possible correlation in the expression of the two molecules was evaluated. As shown in Fig. 6B and C, there was a strict positive correlation between both *RORC2* and *MSC* with *PPP2R2B* mRNA expression. This observation prompted us to investigate whether forced MSC expression in PB-derived classic Th1 cells by lentiviral vector was able to induce upregulation of *PPP2R2B* mRNA expression. As shown in Fig. 6D, *MSC*-, but not control-lentivirus transduction, induced high *PPP2R2B* mRNA expression in classic Th1 cells.

In order to understand whether the high *PPP2R2B* mRNA levels found in Th17 cells may account for their impaired STAT5B ser193 phosphorylation, we stimulated the cells with IL-2 in the presence or in the absence of the total PP2A inhibitor, calyculin A. As shown in Fig. 7A, pretreatment of Th17 cells with calyculin A significantly increased STAT5B ser193 phosphorylation upon IL-2 stimulation. In addition, calyculin A restored STAT5B ser193 phosphorylation in response to IL-2 also in MSC-transduced Th1 cells (Fig. 7B). More importantly, inhibition of *PPP2R2B* with specific siRNA, but not with siRNA control (Fig. 7C), significantly increased the STAT5B ser193 phosphorylation in Th17 cells ($n = 3$ clones) (Fig. 7D).

PP2A controls STAT3 activity in human Th17 cells, but independently of PPP2R2B

STAT3 activity is controlled by phosphorylation on Tyr705, which promotes nuclear translocation and DNA binding, and by phosphorylation on Ser727, that instead has an inhibitory effect since promotes Tyr705 dephosphorylation. It is already known that PP2A favors STAT3 activity by dephosphorylating STAT3 Ser727, and that inhibition of PP2A is associated to reduced Tyr705 phosphorylation upon cytokine triggering, reduced STAT3 DNA binding and its relocation from the nucleus to the cytoplasm [17]. Based on these findings, we hypothesized that the high PP2A activity observed in Th17 cells may not only be involved in inhibiting STAT5B, but also in favoring STAT3, which plays a crucial role in Th17 development and/or maintenance. In order to support this hypothesis, we analyzed STAT3 Ser727 and Tyr705 phosphorylation in response to IL-23 in presence or in absence of the PP2A inhibitor calyculin A. As shown in Fig. 8A, STAT3 Ser727 phosphorylation was not affected by the stimulation with IL-23. However,

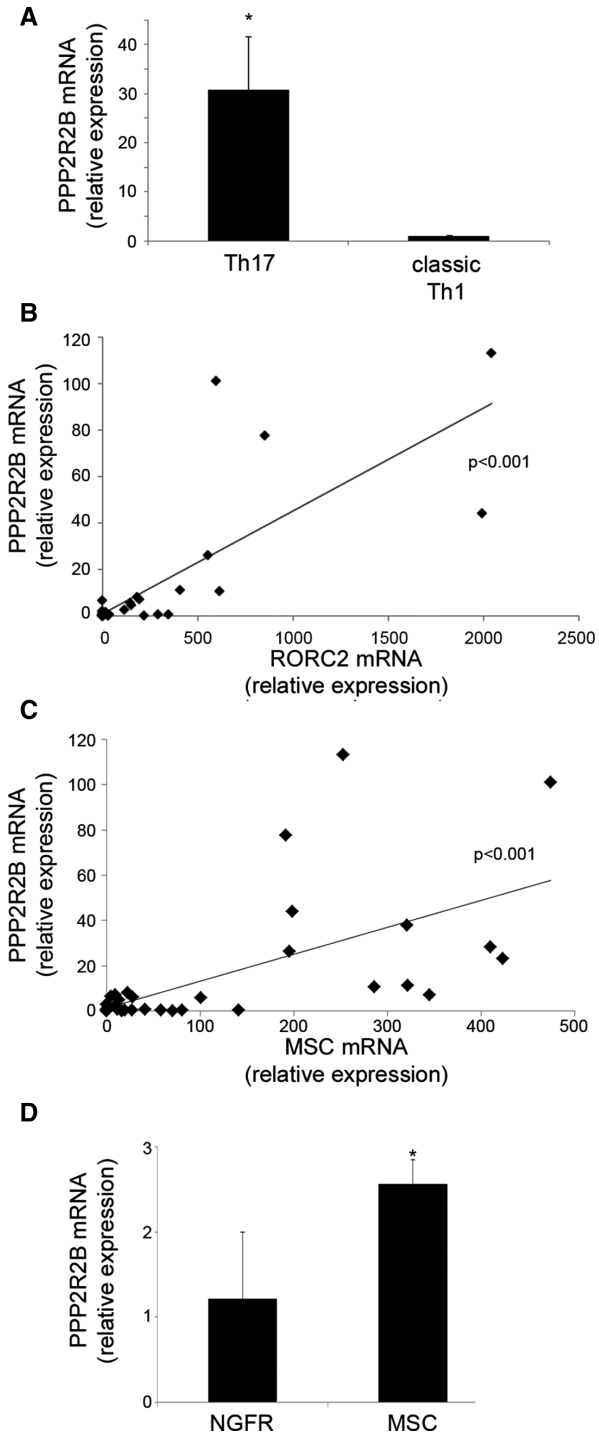

Figure 6. PPP2R2B is more expressed in Th17 cells and is RORC2- and MSC-dependent. (A) Real-time quantitative PCR evaluation of PPP2R2B expression in 10 Th17 and 10 classic Th1 clones. Data are presented as mean of mRNA expression (normalized on GAPDH) + SE. Statistical significance was determined using Student's unpaired *t*-test: $^{*}p \leq 0.05$. (B, C) PPP2R2B mRNA correlation with (B) RORC2 mRNA and (C) MSC mRNA was performed. mRNA levels were normalized on GAPDH. Statistical significance was determined using Pearson's correlation: $p \leq 0.001$. (D) Real-time quantitative PCR evaluation of PPP2R2B expression in 10 NGFR- and 10 MSC-transduced classic Th1 cell lines. Data are presented as mean of mRNA expression (normalized on GAPDH) + SE. Statistical significance was determined using Student's paired *t*-test: $^{*}p \leq 0.05$.

in presence of the PP2A inhibitor, phosphorylation levels of STAT3 Ser727 significantly increased independently of the addition in culture of IL-23 (Fig. 8A). More importantly, the IL-23-induced STAT3 Tyr705 phosphorylation was significantly impaired by the addition in culture of calyculin A (Fig. 8B). These findings support the hypothesis that PP2A controls STAT3 activity. However, given the selective expression of the PPP2R2B regulatory subunit observed in Th17 cells and its importance in regulating STAT5B activity, we wondered whether it might be also responsible for the PP2A-mediated regulation of STAT3 Ser727 phosphorylation. For this reason, we transfected Th17 cells with scramble (NT) or *PPP2R2B*-specific siRNA and we evaluated STAT3 Ser727 and Tyr705 phosphorylation in response to IL-23 signaling. As shown in Fig. 8C, inhibition of *PPP2R2B* mRNA in Th17 cells with specific siRNA did not increase STAT3 Ser727 phosphorylation if compared to the control, and this allowed optimal STAT3 Tyr705 phosphorylation in response to IL-23 stimulation (Fig. 8D). These data clearly demonstrate that STAT3 activity in Th17 cells is regulated by PP2A, but not through the regulatory subunit PPP2R2B.

Overexpression of MSC in human Treg cells inhibits Foxp3 expression

It has been recently shown that MSC is involved in murine iTreg cell development. Upon stimulation of naïve T cells in the presence of TCR triggering and TGF-β, MSC is rapidly upregulated and participates to iTreg phenotype acquisition by suppressing the Th2 program. This occurs by physical interaction with GATA3 transcription factor, leading to its inactivation and thus to blockade of Th2 associated genes expression [18]. Of note, very low levels of MSC expression were found in thymic Treg cells compared with that in iTreg cells, suggesting the involvement of a different molecular machinery in regulatory cell phenotype acquisition and maintenance. In light of these findings, we sorted peripheral human $CD4^{+}CD25^{high}$ Treg cells, to check whether also in the human setting MSC is important for Treg cells. RT-PCR analysis revealed low MSC mRNA transcripts in Treg cells, if compared with that in resting Th17 cells (Fig. 9A). Accordingly, PPP2R2B mRNA levels in Treg cells were lower than in Th17 cells (Fig. 9B). Stimulation of Treg cells with IL-2 showed their capacity to appropriately phosphorylate STAT5B Ser193, in agreement with the pivotal role of this signaling pathway in maintaining high levels of the master transcription factor Foxp3 (Fig. 9C). Thus, we decided to force MSC expression in PB-derived $CD4^{+}CD25^{high}$ Treg cells by lentiviral approach. As expected, we found higher MSC mRNA levels in MSC- than in control-lentivirus transduced cells (Fig. 9D). MSC induction was accompanied by a significant upregulation of PPP2R2B mRNA levels (Fig. 9E) and by lower phosphorylation of STAT5B Ser193 upon IL-2 signalling (Fig. 9F). In order to investigate whether reduced STAT5B Ser193 phosphorylation lead to its functional inactivation, Foxp3 expression in Treg cells was evaluated upon forced induction of MSC. Flow cytometric analysis revealed a significantly lower MFI of Foxp3 in MSC- than in control-lentivirus transduced cells (Fig. 9G).

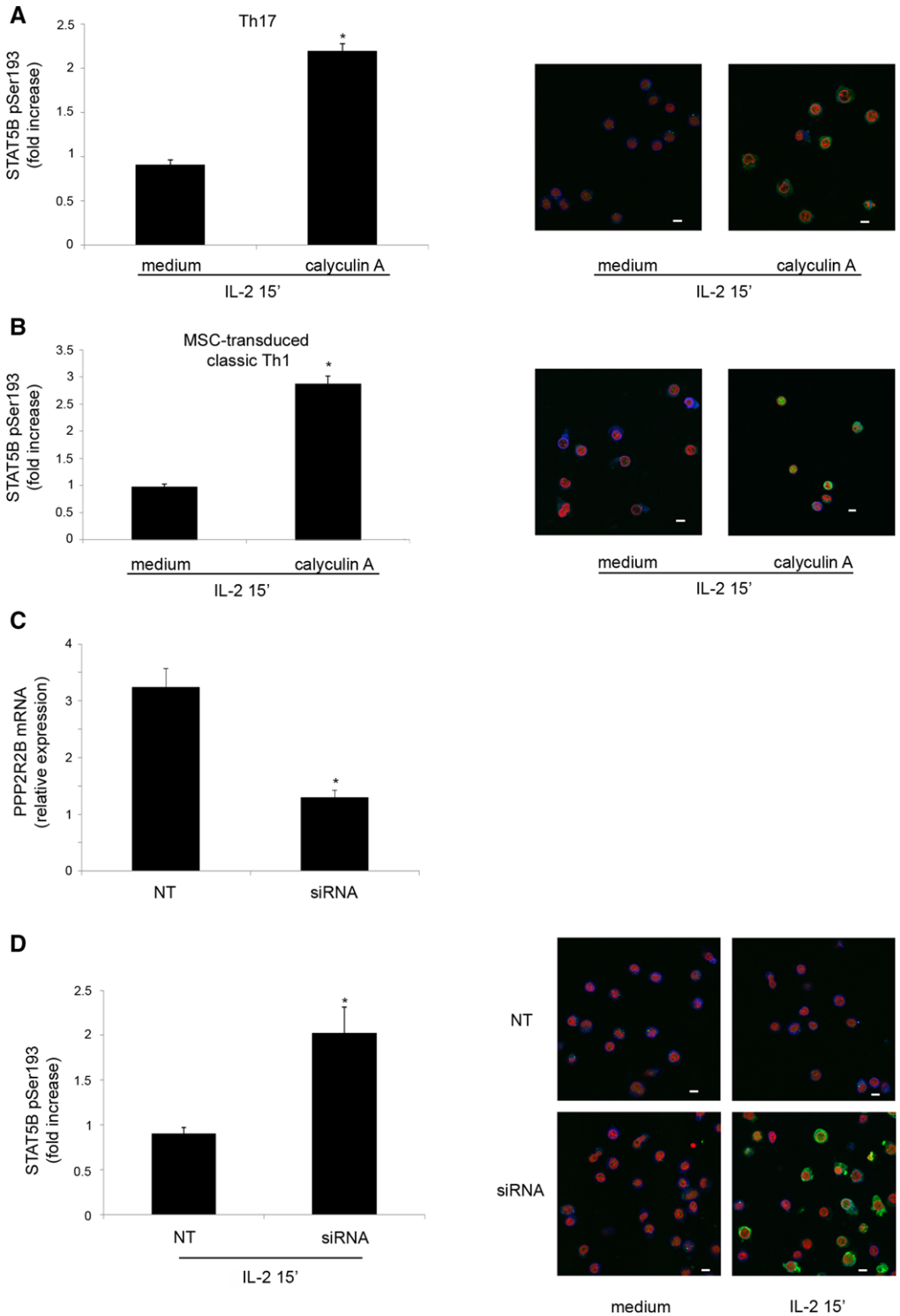

Figure 7. PP2A inhibition leads to increased STAT5B Ser193 phosphorylation both in Th17 and MSC-transduced classic Th1 cells STAT5B Ser193 phosphorylation upon PP2A inhibition was evaluated in Th17 and MSC-transduced Th1 cells (A) 3 Th17 clones and (B) 3 MSC-transduced classic Th1 cell lines were subjected to IL-2 stimulation (15′), in the presence or absence of calyculin A. (A, B) Phosphorylation of STAT5B Ser193 was evaluated by confocal microscopy (scale bars 5 μm). Results are expressed as fold change of MFI of stimulated versus unstimulated. Statistical significance was determined using Student's paired *t*-test: $^{*}p \leq 0.05$. (C) Real-time quantitative PCR evaluation of PPP2R2B mRNA expression in three Th17 clones after 72 h transfection with PPP2R2B-specific and control (NT)-siRNA. Data are presented as mean of mRNA expression (normalized on GAPDH) + SE. Statistical significance was determined using Student's paired *t*-test: $^{*}p \leq 0.05$. (D) Phosphorylation of STAT5B (Ser193) in three Th17 clones transfected with PPP2R2B-specific and control-siRNA induced by IL-2 stimulation (15′). Results are expressed as fold change of MFI of stimulated versus unstimulated. Statistical significance was determined using Student's paired *t*-test: $^{*}p \leq 0.05$. Confocal microscopy images are merged signals of CD3 (blue), TOPRO (red), STAT5B pSer193 (green) (scale bars 5 μm).

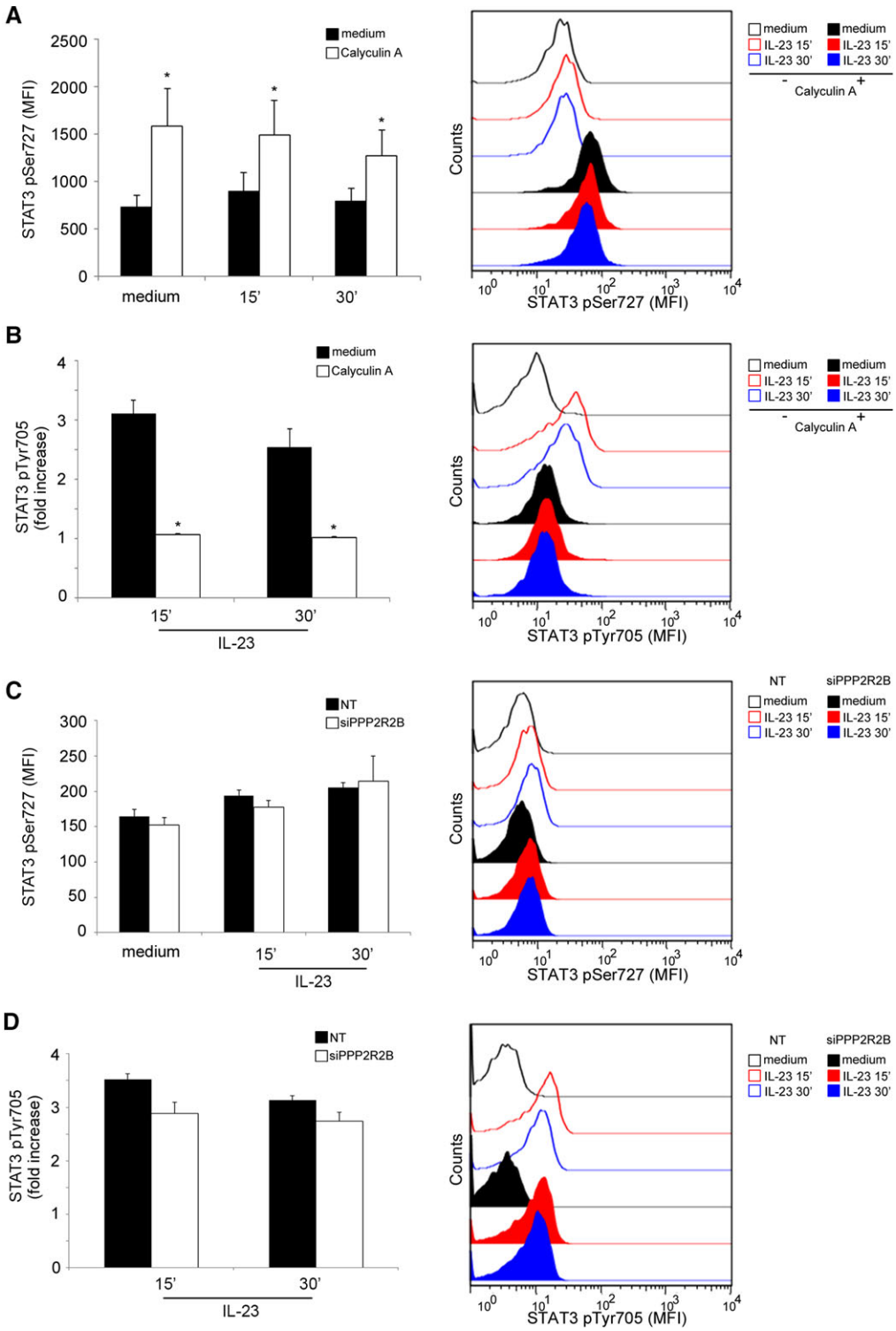

Figure 8. PP2A controls STAT3 activity in a PPP2R2B-independent manner (A, B) 3 Th17 clones cultured in medium alone (black columns) or in the presence of PP2A inhibitor calyculin A (white columns) were subjected to 15′ and 30′ of IL-23 stimulation. Phosphorylation levels of (A) STAT3 Ser727 or (B) STAT3 Tyr705 were evaluated by flow cytometry. (C, D) 3 Th17 clones were subjected to transfection with either control (NT)- (black columns) or PPP2R2B-specific (white columns) siRNA. Phosphorylation of (C) STAT3 Ser727 or (D) STAT3 Tyr705 were evaluated. Results are expressed as kinetics of MFI + SE (A, C) or as MFI + SE fold increase over unstimulated cells (B, D). Representative histogram plots for each experiment are shown (right). Statistical significance was determined using Student's paired *t*-test: $^{*}p \leq 0.05$.

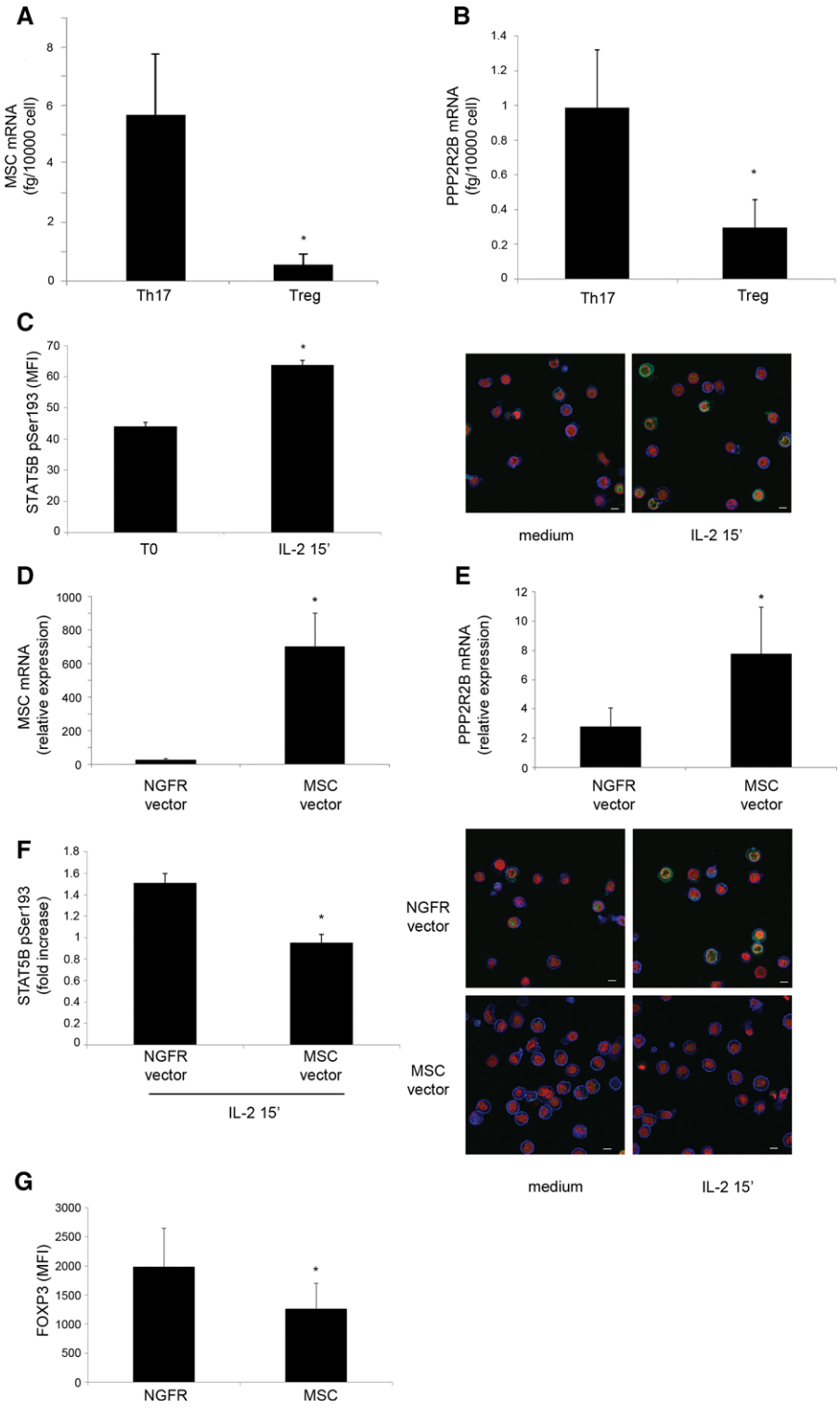

Figure 9. MSC is not expressed by human Treg cells and its forced induction inhibits Foxp3 expression (A, B) five Th17 and four $CD4^+CD25^{high}$ (Treg) cell populations were ex vivo sorted from nine different buffy coats. Real-time quantitative PCR evaluation of (A) Musculin and (B) PPP2R2B gene expression was performed. Data are presented as mean of mRNA fentograms from 10 000 cells + SE. Statistical significance was determined using Student's unpaired *t*-test: $^*p \leq 0.05$. (C) Four $CD4^+CD25^{high}$ (Treg) cell lines established from ex vivo sorted cells was subjected to 15' IL-2 stimulation. Phosphorylation of STAT5B Ser193 was evaluated by confocal microscopy. Results are expressed as MFI + SE (left image). A representative confocal microscopy image of one of the cell lines analyzed is shown (right), with merged signals of CD3 (blue), TOPRO (red), STAT5B pSer193 (green) (scale bars 5 μm). Statistical significance was determined using Student's paired *t*-test: $^*p \leq 0.05$. (D, E) Real-time PCR evaluation of (D) Musculin and (E) PPP2R2B expression in four Musculin and NGFR control-transduced Treg cell lines. Data are presented as mean of mRNA expression (normalized on GAPDH) + SE. Statistical significance was determined using Student's paired *t*-test: $^*p \leq 0.05$. (F) Four $CD4^+CD25^{high}$ (Treg) cell populations transduced with MSC- or NGFR control-vector were evaluated for phosphorylation of STAT5B Ser193 upon 15' IL-2 stimulation, by confocal microscopy. Confocal microscopy images are merged signals of CD3 (blue), TOPRO (red), STAT5B pSer193 (green) (scale bars 5 μm). Results are expressed as fold change of MFI + S E of stimulated versus unstimulated. Statistical significance was determined using Student's paired *t*-test: $^*p \leq 0.05$. (G) Foxp3 expression was evaluated by flow cytometry analysis in four Musculin and NGFR-control transduced Treg cell lines. Results are expressed as MFI + SE. Statistical significance was determined using Student's paired *t*-test: $^*p \leq 0.05$.

Discussion

We have previously shown that human Th17 cells, despite their well-known pathogenicity, have a lower frequency than Th1 cells at sites of inflammation. The reasons for this rarity can be identified in (i) the tendency of these cells to shift their phenotype towards Th1 in presence of an inflammatory microenvironment, and (ii) in their inability to appropriately clonally expand upon antigen recognition. In a previous study, we found that the control of Th17 cell expansion is mediated by a RORγt-dependent mechanism, which involves the expression of IL4I1, a phenylalanine oxydase that is responsible for CD3 molecules downregulation. In

the same study, we also found that Th17 cells were also impaired in ensuring an appropriate sensitivity to IL-2 stimulation, if compared to Th1 cells, although the precise mechanisms involved in this defect were not extensively investigated.

The functional role of MSC in T lymphocytes, to date, has not been clarified. MSC expression by Th17 cells was epigenetically regulated through DNA methylation, appeared to be RORγt-dependent, and its forced expression in Th1 cells resulted in a strong inhibition of their responsiveness to IL-2. In order to understand how MSC can interfere with the IL-2 response, we decided to look at the different steps by which IL-2 is known to mediate signaling events on IL-2 target genes. We observed no abnormalities in the initial steps of the signaling cascade, but we found that in *MSC*-transduced Th1 cells STAT5B displayed a reduced phosphorylation at Ser193, a regulatory site that is important to ensure proper DNA binding and transcriptional activity. The same phosphorylation defect upon IL-2 triggering was present also in Th17, when compared to Th1, cells. Thus, MSC expression is followed by reduced IL-2 signaling because of a reduced phosphorylation of STAT5B Ser193. Moreover, we found that this impairment is due to the MSC-mediated upregulation of PPP2R2B, a regulatory subunit that directs the phosphatase activity of the PP2A enzyme on STAT5B Ser193. Inhibition of total PP2A via calyculin A or, more importantly, selective inhibition of PPP2R2B via siRNA, was able to restore STAT5B Ser193 phosphorylation upon IL-2 signaling in human Th17 cells. By this way, impaired STAT5B DNA-binding capacity leads to inappropriate expression of genes involved in cell growth and proliferation.

Previous data in the literature show that PP2A regulates also the activity of STAT3, which plays a critical role in favoring Th17 cell development and maintenance. In particular, PP2A is involved in the dephosphorylation of STAT3 Ser727, that is fundamental to guarantee proper STAT3 Tyr705 phosphorylation upon cytokine triggering, a mandatory event for STAT3 translocation into the nucleus and DNA binding [17]. Our data confirm these findings, since PP2A inhibition via calyculin A treatment in Th17 cells increased STAT3 pSer727 and in parallel reduced STAT3 pTyr705 upon IL-23 triggering. However, this activity seems to be independent by PPP2R2B, since its specific silencing is not able to increase the phosphorylation of STAT3 Ser727 and to decrease that of STAT3 Tyr705.

The role of STAT5B Ser193 in controlling cell proliferation is not restricted to Th17 cells but can be extended to all PB mononuclear cells (PBMNC) since its phosphorylation has been observed in these cells in response to several γ-chain cytokines such as IL-2, IL-7, IL-9, IL-15. In agreement with this, alterations of STAT5 are involved in oncogenesis and it has been shown to be constitutively activated in myeloid, lymphoid, and erythroid leukemia [15]. Recent evidences show that Ser193 can be one of the sites responsible for STAT5B continuous activation since it is constitutively phosphorylated in several lymphoid tumor cell lines, as well as in primary leukemia and lymphoma patient tumor cells [15]. Of note, it would be of particular interest understanding whether in these malignancies the constant phosphorylation of STAT5B Ser193 is maintained thanks to a loss of MSC and/or PPP2R2B activity, thus identifying these genes as members of the oncosuppressor family. In line with this hypothesis, it has been shown that *PPP2R2B* is commonly epigenetically silenced in human colorectal cancer [19].

In addition to cell-cycle control, the data presented provide novel tools for better understanding the development and the maintenance of the T-cell phenotype since both STAT5 and STAT3 play pivotal roles in these processes. Indeed, it has already been shown that these STAT family members compete for binding to several DNA regions, and their balance is important to direct the development and the maintenance of two opposite T-cell programs. On one side, STAT3 prevalence favors Th17 cell differentiation, allowing *RORC2* and *IL17A* gene expression; on the other, STAT5 prevalence inhibits the Th17 program by inhibiting *IL17* locus expression, while favoring the development of Treg cells, with the upregulation of *FOXP3* and *IL2RA* genes [20, 21]. Thus, by controlling the activation status of these two competing STAT proteins, PP2A enzyme may play a central role in controlling T-cell fate. Supporting this concept, we have shown that MSC is not expressed by human Treg cells, and that its forced overexpression leads to *PPP2R2B* upregulation, STAT5B Ser193 dephosphorylation and inhibition of DNA-binding capacity that is revealed by a significant reduction of Foxp3 protein expression. In agreement with our observations, recent data in the literature show that in mice STAT5B has a dominant role over STAT5A in controlling Foxp3 expression, since in vitro induced Treg cells from *Stat5b*$^{-/-}$ mice exhibit lower levels of both *Foxp3* mRNA and protein if compared to *STAT5a*$^{-/-}$ mice. Moreover, in vivo induced Foxp3^{+} Treg cells from the same *Stat5b*$^{-/-}$ mice have lower expression of IL-2rα and reduced suppressive capacity, when compared to *Stat5a*$^{-/-}$ Tregs [22]. In addition, human studies support the notion that STAT5B is fundamental for the expression of Foxp3 and IL-2Rα, since STAT5B$^{-/-}$ patients (with normal STAT5A function) are characterized by Treg cells that are both reduced in numbers and decreased in suppressive function [23]. Musculin was recently identified also in murine iTreg: while both thymic Treg (tTreg) cells and iTreg cells require IL-2 for their maintenance and expansion via STAT5 signaling, iTreg cells develop by stimulation of naïve T cells with TGF-β that results in the induction of Foxp3 expression via the Smad3 signaling; early musculin upregulation, TGF-β dependent, has been demonstrated to be responsible for Th2 polarization repression; instead, thymus derived murine Treg show very low MSC expression [18]. Our data show that human PB-derived CD4^{+}CD25^{high} Treg cells do not express MSC, and its forced induction leads to Foxp3 downregulation. These differences may be due to different mechanisms operating in the two species, human, and mouse, but also because the experimental settings are not comparable due to the absence in humans of selection markers such as murine Neuropilin that allow to distinguish iTreg from tTreg cells. Another transcription factor whose expression is strictly controlled by the STAT3-STAT5 balance is BCL6, the master regulator of Tfh cells differentiation. Again, STAT3 dominance favors BCL6 expression, while STAT5 has inhibitory effects on this gene [24]. In agreement with our findings, it has recently been shown that murine Tfh cells express *Msc*, thus suggesting that also

in these cells the molecular axis MSC-PPP2R2B is active and is involved in inhibiting STAT5 activity in favor of STAT3 [12].

In conclusion, the emerging scenario depicts the existence of a complex network of signaling proteins that is deputed to the fine regulation of the activation status of STAT3 and STAT5 transcription factors. PP2A enzyme seems to play a key role in this network, thus further deepening of the mechanisms and the actors that play a role in regulating its activity might be of great interest for better understanding how T cells make decisions regarding their phenotype.

Materials and methods

The authors acknowledge the recently published Minimum Information about T-cell Assays (MIATA) Guidelines and have provided detailed information in accordance with MIATA.

Subjects

PB samples were obtained from eight healthy donors. SF samples were collected from four JIA patients. UCB samples were obtained from three donors. The procedures followed in the study were in accordance with the ethical standards of the Regional Committee on Human Experimentation.

Reagents

The medium used was RPMI 1640 (Seromed, Berlin, Germany), supplemented with 2 mM L-glutamine, 1% nonessential amino acids, 1% pyruvate, 2 × 10–5 M 2-mercaptoethanol (2-ME) (all from Gibco Laboratories, Grand Island, NY), and 10% FCS (Euroclone). Unlabeled or flurochrome-conjugated anti-CD3, CD4, CD8, CD161, CCR6, CD271, IFN-γ, isotype-matched control mAbs were from BD Biosciences (Mountain View, CA). Flurochrome-conjugated anti-IL-17 mAbs were from eBiosciences (San Diego, CA). PE-Cy7-conjugated CD161 was from (Miltenyi Biotec, Bergisch Gladbach). Flurochrome-conjugated anti-CXCR3 mAbs were from R&D System. Phorbol 12-myristate 13-acetate (PMA), ionomycin, brefeldin A, and saponin were from Sigma Aldrich Co. (St. Louis, MO).

T-cell recovery and expansion

MNC suspensions were obtained from PB, SF, and UCB by centrifugation on Ficoll–Hypaque gradient; cell counting was performer with a hemocytometer. PB $CD4^+$ T cells were negatively selected by high-gradient magnetic cell sorting (Miltenyi Biotec), as previously described [25] and were then further divided into $CD161^+$ and $CD161^-$ by immunomagnetic cell sorting. PB $CD4^+CD161^+$ and $CD4^+CD161^-$ T-cell population were further subdivided in $CCR6^+$ and $CCR6^-$ cell fractions by FACSAria (BD Biosciences). PB $CD4^+CD161^+CCR6^+$ and $CD4^+CD161^-CCR6^-$ cell lines were then cultured under limiting dilution in order to obtain Th17, nonclassic Th1, and Th1 clones, respectively, classified by flow cytometry for intracellular staining of IL-17 or IFN-γ cytokines [3, 6]. PB $CD4^+CD161^-CCR6^-$ were also FACS enriched for $CXCR3^+$ expression to obtain classic Th1 cell polyclonal population (Supporting Information Fig. 4). PB $CD4^+CD161^+CCR6^+$ were further divided in $CXCR3^+$ and $CXCR3^-$ by FACS to obtain nonclassic Th1 and Th17 cell polyclonal cell lines, respectively. Treg cells were obtained by FACSAria as CD25 high expressing cells starting from negatively selected $CD4^+$ T population. UCB $CD4^+$ T cells, from three samples, negatively selected by high-gradient magnetic cell sorting, were further divided into $CD161^+$ and $CD161^-$ T-cell fractions by FACSAria.

Cytokine secretion assay

PB and SF $CD4^+$ T cells were negatively selected by high-gradient magnetic cell sorting and further divided into $CCR6^+$ and $CCR6^-$ cells by immunomagnetic cell sorting, then were stained with anti-CD161 PE-Cy7, stimulated with PMA-ionomycin, recovered after 3 and half hours, washed and then stained with IFN-γ and IL-17 catch reagents (Miltenyi Biotec), following manufacturer's instructions. Following additional 45 min of incubation (37°C, 5% CO2) cells were stained with anti-CD3-Pacific Blue, -IL-17-APC, and -IFN-γ-FITC, analyzed and sorted by FACSAria. PB and SF samples were divided into $CD4^+$ $CCR6^+$ $CD161^+$ IL-17^+IFN-γ^-, $CD4^+$ $CCR6^+$ $CD161^+$ IL-17-IFN-γ^+, $CD4^+$ $CCR6^-$ $CD161^-$ IL-17-IFN-γ^+ T cells.

RNA isolation, cDNA synthesis, and real-time quantitative RT-PCR

Total RNA was extracted by using the RNeasy Micro Kit (Qiagen, Hilden, Germany) and treated with DNase I to eliminate possible genomic DNA contamination. RNA reverse transcription was performed with Taqman Gold kit (Thermo Fisher Scientific). Briefly, for the analysis of each gene expression, total mRNA recovered from 10 000 cells was reverse transcribed and then subjected to RT-PCR amplification. Ct values were then transformed into fentograms of cDNA using a standard curve. For in vitro cultured cells, cDNA fentograms were then normalized on GAPDH cDNA fentograms, in order to exclude possible activation-dependent differences (relative expression). Primers and probes used were purchased from Thermofisher.

Western blot analysis

T-cell lysates were prepared in lysis buffer (RIPA buffer: 25 mM Tris-HCl pH7.6, 150 mM NaCl, 1% NP-40, 1% sodium deoxycholate, 0.1% SDS, and 5 mM EDTA) containing a protease- and phosphatase-inhibitor mixture (Pierce). Proteins were quantified by Bradford Assay, then equivalent amounts were separated by SDS-PAGE on a 4–20% polyacrylamide gel (Bio-Rad, USA) for

2 hours at 120 V, transferred to a nitrocellulose membrane for 16 h at 30 V, and finally blocked in 5% milk for 1 hour at room temperature. Proteins were detected by anti-human MSC (sc9555; clone N20 Santa-Cruz biotechnology), anti-human STAT5b, anti-human STAT5a (abcam: ab178941, ab32043) or anti-human STAT5b phospho-Ser193 (gently provided by Robert A. Kirken University of Texas at El Paso) administered for 18 hours and followed by incubation with horseradish peroxidase–conjugated anti-rabbit, anti-goat Ab (Santa-Cruz biotechnology) for 1 hour at room temperature. β−Actin was used as protein loading control and detected by 1 hour room temperature staining with horseradish peroxidase-conjugated mouse anti-human β−Actin (Sigma Aldrich). An enhanced chemiluminescent substrate (GE Healthcare) for detection of HRP was used for visualization. Immunoblot films were digitized and analyzed using ImageJ (National Institutes of Health). Optical density (OD) of the immunoreactivity of interest, e.g. STAT5B, was normalized to β-actin OD. All Western blot densitometry data are normalized for the loading control β-actin, and expressed as "relative optical density."

Confocal microscopy

For MSC evaluation cells were first incubated for 30 min with biotin-NGFR mAb or with a control isotype, washed, and incubated with Streptavidin-488 conjugated. Cells were then fixed in formaldehyde, permeabilized with cold methanol (Sigma), and incubated with rabbit IgG (1 mg/mL). Finally, cells were stained with an anti-MSC Ab (goat IgG, Santa Cruz, 5 μg/mL) or control isotype (goat IgG, Santa Cruz, 5 μg/mL) overnight. The day after, detection was performed with Alexa Fluor 546-conjugated anti-goat IgG (2 μg/mL), in buffer containing TOPRO-3 dye (0.2 μM) for nuclear counter staining. For STAT5B pSer193 detection, cells were stimulated with or without IL-2 (50 U/mL), then fixed in formaldehyde and permeabilized with 0.1% Triton (Sigma), and incubated with goat serum (1 mg/mL). Cells were stained with rabbit polyclonal IgG anti-Stat5b pSer193 Ab (Robert A. Kirken University of Texas at El Paso 10 μg/m) or anti-Stat5b (Abcam) and anti-CD3 (mouse IgG1, BD, 10 μg/mL); detection was done with Alexa Fluor 488 anti-rabbit IgG and Alexa Fluor 546 anti-mouse-IgG1 (2 μg/mL both), in buffer containing TOPRO-3 dye (0.2 μM). Microscopic images were taken by a LSM 510 META Zeiss confocal microscope system (Carl Zeiss Inc., Jena, Germany), using 40X oil immersion lens, corresponding to a 400X magnification. For images analysis Confocor 2 (Zeiss) software was used. Scale bars = 5μm.

DNA methylation analysis

DNA methylation was evaluated by bisulfite cloning and sequencing approach. Genomic DNA was extracted with the DNA Blood Mini Kit (QIAGEN, Hilden, Germany) as previously described (Mazzoni 2015) followed by bisulfite conversion with the EpiTect Bisulfite Kit (Qiagen), according to the manufacturer's instructions. Bisulfite treated DNA was PCR amplified by using bisulfite-specific primers F: 5′AATTTATTAAATATAATAGTAAGGATTTTT R: 5′ AATTTACAAAACTTAAAACTAAACC and then cloned into pCR2.1 vector (Invitrogen). Cloned products were then transformed into chemically competent *E. coli* TOP10 cells (Invitrogen). Plasmid DNA from at least 15 colonies for each population was recovered and then sequenced by Sanger sequencing (GATC Biotech AG, Constance, Germany). Finally, sequences were analyzed with BISMA software (Rohde 2010).

T-cell proliferation assay

A total of 0.5×10^5 T cells were cultured for 3 days with anti-CD3-CD28 mAbs (5 μg/mL each), in presence or absence of IL-2 (50 IU/mL) or with IL-2 alone. On day 3, cells were pulsed for 8 h with 0.5 μCi of 3H-TdR (Perkin Elmer), then harvested, and radionuclide uptake was measured by scintillation counting.

Chromatin immunoprecipitaion

ChIP was performed essentially as described (Nebbioso et al., 2005) with anti-human RORC (clone ab41941, Abcam; Cambridge, UK) on Th17 cell clones after 6 h stimulation with anti-CD3-CD28 mAbs. The quantitative PCR, performed in an abi 7500 thermal Cycler, was carried out with a set of primer: 5′ TAG ATT GTG TAT TGA AGA GCG A 3′- 5′ AGA CGT ACT TAT CCC CTG AC 3′; 5′ TGG CAT TTG GTC ACC TCC TTC 3′-5′ ATA AGA TAA AAA TAA AGG CTG TA 3′; 5′TTCACATTGTCCCAGAACCA3′-5′ACAAAGGAGCACCCTGAATG3′. After amplification, data were analyzed according a standard method (DDCt calculation) and controlled against a no-Ab input and plotted as percentage of total chromatin input.

Lentivirus transduction

PB derived CD4+CD161−CCR6−CXCR3+ cells, and UCB derived CD4+CD161+ cells were activated with irradiated APCs plus anti-CD3 mAb (1 μg/mL). After 16 h, pCCL EF1α NGFR or pCCL EF1α NGFR RORC2 or pCCL EF1α NGFR MSC lentivirus were added at a multiplicity of infection of 10 and cells were spinoculated at 1200 × g, 26°C for 2 h. Transduced T cells were kept in culture with IL-2 (100 U/mL, Eurocetus, Italy), purified after 10 days with anti-NGFR-PE (BD Biosciences) plus anti-PE microBeads (Miltenyi Biotec); purities greater than 98% being consistently achieved, and then expanded with irradiated APCs, anti-CD3 plus IL-2 for additional 3 weeks.

siRNA delivery and gene silencing

One hundred seven cells of Th17 cell clones were transiently nucleofected with 3 μM of hRORC-siRNA (siGENOME SMARTpool, GE

Healthcare Dharmacon) or with 1 μM PPP2R2B-siRNA (Silencer® siRNAs, Ambion, Thermo Fisher Scientific) by electroporation with the Amaxa Nucleofector (program T-020; Amaxa Biosystems) with the Human T Cell Nucleofector Kit (Lonza Basel, Switzerland). siGENOME Non-Targeting siRNA (NT) Control Pools or Silencer® Negative Control were used as negative control of hRORC-siRNA or hPPP2R2B-siRNA, respectively. Cells were harvested at 72, 96, and 120 h for mRNA evaluation by RT-PCR, STAT5B Ser193 phosphorylation status by confocal microscopy and STAT3 phosphorylation by flow cytometry.

Phospho-protein assays

Phosphorylated proteins were evaluated by PhosFlow (BD Biosciences) intracellular cell staining protocol following manufacturer's instructions. Briefly, cells were stimulated with IL-2 (50 IU/mL) or triggered with mAbs anti-CD3/CD28 mAbs and at different time point were fixed in CytoFix Buffer I for 10 min at 37°C, permeabilized 30 min on ice with Perm Buffer III and stained with the specific Abs: fluorochrome-conjugated anti-phospho-STAT5 (Tyr694), CD3ζ (Tyr142) (BD Biosciences), or S6ribo (Ser235 and 236) (Cell Signaling). Stained cells were then analyzed on a BDLSRII cytometer (BD Biosciences). Histogram plots were obtained using FlowJo software (Tree Star,Oregon, USA).

Microarray

Gene expression profiles on human Th1 and Th7 clones were assessed by cDNA microarray technique using One Color Microarray Quick Labeling kit (Agilent Technologies, Cernusco s/N, MI, Italy), as previously described (Santarlasci 2012). The microarray data are available in the Gene Expression Omnibus database (http://www.ncbi.nlm.nih.gov/gds) under the accession number GSE30664

Statistics

Student *t*-test was used for mRNA expression analysis, MFI analysis of flow cytometry and confocal microscopy, immunoblot densitometry, and 3H-TdR uptake experiments. Mann–Whitney test was used for DNA methylation and ChIP studies. *p* values of 0.05 or less were considered significant. Pearson's correlation coefficients were used to calculate the correlations.

Authors' contribution

A.M., M.C., M.C.R., B.R., L.M., G.B., V.S., and G.M. performed the experiments and collected the data, V.S., A.M., M.C.R., M.C., M.R., and F.A. analyzed data, A.M., M.C., V.S., and F.A. wrote the manuscript. F.A., R.C., L.C., F.L., and R.D.P. supervised the manuscript. S.R., E.M., and F.A. gave the final approval of the version of the manuscript. All authors read and approved the final manuscript.

Acknowledgments: The experiments reported in this paper have been supported by funds of the Italian Ministry of Education (PRIN) to F.A., the Ente Cassa di Risparmio di Firenze to F.A., Associazione Italiana Ricerca sul Cancro (AIRC) to E.M.

Conflict of interest: The authors declare no financial or commercial conflict of interest.

References

1 **Zhu, J. and Paul, W. E.**, Peripheral CD4+ T-cell differentiation regulated by networks of cytokines and transcription factors. *Immunol. Rev.* 2010. **238**: 247–262.

2 **Annunziato, F., Santarlasci, V., Maggi, L., Cosmi, L., Liotta, F., and Romagnani, S.**, Reasons for rarity of Th17 cells in inflammatory sites of human disorders. *Semin. Immunol.* 2013. **25**: 299–304.

3 **Annunziato, F., Cosmi, L., Santarlasci, V., Maggi, L., Liotta, F., Mazzinghi, B., Parente, E. et al.**, Phenotypic and functional features of human Th17 cells. *J. Exp. Med.* 2007. **204**: 1849–1861.

4 **Maggi, L., Cimaz, R., Capone, M., Santarlasci, V., Querci, V., Simonini, G., Nencini, F. et al.**, Brief report: etanercept inhibits the tumor necrosis factor alpha-driven shift of Th17 lymphocytes toward a nonclassic Th1 phenotype in juvenile idiopathic arthritis. *Arthritis Rheumatol.* 2014. **66**: 1372–1377.

5 **Annunziato, F., Cosmi, L., Liotta, F., Maggi, E., and Romagnani, S.**, Defining the human T helper 17 cell phenotype. *Trends Immunol.* 2012. **33**: 505–512.

6 **Maggi, L., Santarlasci, V., Capone, M., Rossi, M. C., Querci, V., Mazzoni, A., Cimaz, R. et al.**, Distinctive features of classic and nonclassic (Th17 derived) human Th1 cells. *Eur. J. Immunol.* 2012. **42**: 3180–3188.

7 **Mazzoni, A., Santarlasci, V., Maggi, L., Capone, M., Rossi, M. C., Querci, V., De, P. R. et al.**, Demethylation of the RORC2 and IL17A in human CD4+ T lymphocytes defines Th17 origin of nonclassic Th1 cells. *J. Immunol.* 2015. **194**: 3116–3126.

8 **Santarlasci, V., Maggi, L., Capone, M., Querci, V., Beltrame, L., Cavalieri, D., D'Aiuto, E. et al.**, Rarity of human T helper 17 cells is due to retinoic acid orphan receptor-dependent mechanisms that limit their expansion. *Immunity* 2012. **36**: 201–214.

9 **Massari, M. E., Rivera, R. R., Voland, J. R., Quong, M. W., Breit, T. M., van Dongen, J. J., de, S. O. et al.**, Characterization of ABF-1, a novel basic helix-loop-helix transcription factor expressed in activated B lymphocytes. *Mol. Cell Biol.* 1998. **18**: 3130–3139.

10 **Mathas, S., Janz, M., Hummel, F., Hummel, M., Wollert-Wulf, B., Lusatis, S., Anagnostopoulos, I. et al.**, Intrinsic inhibition of transcription factor E2A by HLH proteins ABF-1 and Id2 mediates reprogramming of neoplastic B cells in Hodgkin lymphoma. *Nat. Immunol.* 2006. **7**: 207–215.

11 **Zhao, P. and Hoffman, E. P.**, Musculin isoforms and repression of MyoD in muscle regeneration. *Biochem. Biophys. Res. Commun.* 2006. **342**: 835–842.

12 **Debuisson, D., Mari, N., Denanglaire, S., Leo, O. and Andris, F.**, Myor/ABF-1 mRNA [corrected] expression marks follicular helper T cells but is dispensable for Tfh cell differentiation and function in vivo. *PLoS One* 2013. **8**: e84415.

13 **Liao, W., Lin, J. X., and Leonard, W. J.**, IL-2 family cytokines: new insights into the complex roles of IL-2 as a broad regulator of T helper cell differentiation. *Curr. Opin. Immunol.* 2011. **23**: 598–604.

14 **Lin, J. X. and Leonard, W. J.**, The role of Stat5a and Stat5b in signaling by IL-2 family cytokines. *Oncogene* 2000. **19**: 2566–2576.

15 **Mitra, A., Ross, J. A., Rodriguez, G., Nagy, Z. S., Wilson, H. L., and Kirken, R. A.**, Signal transducer and activator of transcription 5b (Stat5b) serine 193 is a novel cytokine-induced phospho-regulatory site that is constitutively activated in primary hematopoietic malignancies. *J. Biol. Chem.* 2012. **287**: 16596–16608.

16 **Haesen, D., Sents, W., Lemaire, K., Hoorne, Y., and Janssens, V.**, The basic biology of PP2A in hematologic cells and malignancies. *Front Oncol.* 2014. **4**: 347.

17 **Woetmann, A., Nielsen, M., Christensen, S. T., Brockdorff, J., Kaltoft, K., Engel, A. M., Skov, S. et al.**, Inhibition of protein phosphatase 2A induces serine/threonine phosphorylation, subcellular redistribution, and functional inhibition of STAT3. *Proc. Natl. Acad. Sci. USA* 1999. **96**: 10620–10625.

18 **Wu, C., Chen, Z., Dardalhon, V., Xiao, S., Thalhamer, T., Liao, M., Madi, A. et al.**, The transcription factor musculin promotes the unidirectional development of peripheral Treg cells by suppressing the TH2 transcriptional program. *Nat. Immunol.* 2017. **18**: 344–353.

19 **Tan, J., Lee, P. L., Li, Z., Jiang, X., Lim, Y. C., Hooi, S. C., and Yu, Q.**, B55beta-associated PP2A complex controls PDK1-directed myc signaling and modulates rapamycin sensitivity in colorectal cancer. *Cancer Cell* 2010. **18**: 459–471.

20 **Laurence, A., Tato, C. M., Davidson, T. S., Kanno, Y., Chen, Z., Yao, Z., Blank, R. B. et al.**, Interleukin-2 signaling via STAT5 constrains T helper 17 cell generation. *Immunity* 2007. **26**: 371–381.

21 **Yang, X. P., Ghoreschi, K., Steward-Tharp, S. M., Rodriguez-Canales, J., Zhu, J., Grainger, J. R., Hirahara, K. et al.**, Opposing regulation of the locus encoding IL-17 through direct, reciprocal actions of STAT3 and STAT5. *Nat. Immunol.* 2011. **12**: 247–254.

22 **Villarino, A., Laurence, A., Robinson, G. W., Bonelli, M., Dema, B., Afzali, B., Shih, H. Y. et al.**, Signal transducer and activator of transcription 5 (STAT5) paralog dose governs T cell effector and regulatory functions. *Elife* 2016. **5**: 1–26.

23 **Jenks, J. A., Seki, S., Kanai, T., Huang, J., Morgan, A. A., Scalco, R. C., Nath, R. et al.**, Differentiating the roles of STAT5B and STAT5A in human CD4+ T cells. *Clin. Immunol.* 2013. **148**: 227–236.

24 **Walker, S. R., Nelson, E. A., Yeh, J. E., Pinello, L., Yuan, G. C., and Frank, D. A.**, STAT5 outcompetes STAT3 to regulate the expression of the oncogenic transcriptional modulator BCL6. *Mol. Cell Biol.* 2013. **33**: 2879–2890.

25 **Cosmi, L., De Palma, R., Santarlasci, V., Maggi, L., Capone, M., Frosali, F., Rodolico, G. et al.**, Human interleukin 17-producing cells originate from a CD161+CD4+ T cell precursor. *J. Exp. Med.* 2008. **205**: 1903–1916.

Abbreviations: **MSC**: Musculin · **OD**: optical density · **ROR**: retinoic acid orphan receptor · **STAT4**: signal transducer and activator of transcription 4 · **UCB**: umbilical cord blood

Full correspondence: Prof. Francesco Annunziato, Department of Experimental and Clinical Medicine, University of Florence, Viale Pieraccini 6 Firenze 50134, Italy
Tel. +39-055-2758337
e-mail: francesco.annunziato@unifi.it

Received: 15/2/2017
Revised: 22/5/2017
Accepted: 9/6/2017
Accepted article online: 14/6/2017

